Anisotropic Intramolecular Backbone Dynamics of Ubiquitin Characterized by NMR Relaxation and MD Computer Simulation

S. F. Lienin, T. Bremi, B. Brutscher,† R. Brüschweiler,* and R. R. Ernst*

Contribution from the Laboratorium für Physikalische Chemie, ETH Zentrum, 8092 Zürich, Switzerland

Received March 25, 1998. Revised Manuscript Received July 23, 1998

Abstract: The anisotropy of rapid fluctuations of the peptide planes in ubiquitin is explored by combined ^{15}N and $^{13}C'$ nuclear spin relaxation measurements and molecular dynamics (MD) computer simulation. T_1, T_2, and NOE data were collected at B_0-field strenghts corresponding to 400 and 600 MHz proton resonance. A 1.5-ns simulation of ubiquitin in an explicit water environment was performed using CHARMM 24. The simulation suggests that, for 76% of the peptide planes, the relaxation-active motion of the backbone ^{15}N and $^{13}C'$ spins is dominated by anisotropic Gaussian axial fluctuations of the peptide planes about three orthogonal axes. The dominant fluctuation axes are nearly parallel to the $C^{\alpha}_{i-1}-C^{\alpha}_{i}$ axes. The remaining peptide planes belong to more flexible regions of the backbone and cannot be described by this type of motion alone. Based on the results of the computer simulation, an analytical 3D GAF motional model (Bremi, T.; Brüschweiler, R. *J. Am. Chem. Soc.* **1997**, *119*, 6672−6673) was applied to the experimental relaxation data. The fluctuation amplitudes of the peptide planes show a significant anisotropy of the internal motion. This analysis demonstrates that a combined interpretation of ^{15}N and $^{13}C'$ relaxation data by a model derived from a computer simulation may provide detailed insight into the fast time-scale backbone dynamics that goes beyond the results of a standard model-free analysis.

1. Introduction

Intramolecular motion of biomolecules is generally anisotropic. The anisotropy can be assessed experimentally and by computer simulations. In X-ray crystallography, for example, it is represented by anisotropic crystallographic *B*-factors.[1] Using NMR relaxation spectroscopy, the possibility to probe anisotropic motion critically depends on the principal axis directions of the dominant relaxation-active interactions. For example, the relaxation of a ^{15}N nucleus of the protein backbone is governed by the (axially symmetric) magnetic dipolar $^{15}N-^{1}H$ coupling and by the ^{15}N chemical shift anisotropy (CSA) interaction, which is, to a good approximation, axially symmetric with the symmetry axis parallel to the $^{15}N-^{1}H$ vector. Thus, fast reorientational motions scale the dipolar $^{15}N-^{1}H$ and the ^{15}N CSA interactions by nearly the same order parameter, S^2.[2] The monitoring of three-dimensional anisotropic motion by NMR relaxation measurements requires rigid fragments with a set of spin interactions that probe different directions in space.

We demonstrate here experimentally that anisotropic intramolecular backbone motion can be characterized by a combined interpretation of relaxation data of $^{13}C'$and ^{15}N nuclei belonging to the same peptide bond. The proposed analysis takes advantage of the fact that the peptide-bond geometry remains, to a good approximation, planar at all times. Thus, the relaxation-active CSA and dipolar interaction tensors have fixed relative orientations. Since their principal axes are generally not parallel, they sample different motional modes, allowing for the exploration of locally anisotropic motion. Previous model calculations have demonstrated the feasibility of this approach.[3] The analysis is applied in this paper to the fully ^{13}C- and ^{15}N-labeled native form of the 76-residue protein ubiquitin (see Figure 1). This system was studied before extensively by homonuclear and heteronuclear NMR.[6−9]

The procedure follows the general protocol originally developed for the characterization of side-chain dynamics and subsequently applied to the characterization of backbone dynamics, exemplified on the cyclic decapeptide antamanide.[3,10] The protocol uses information gained from molecular dynamics (MD) computer simulations and from analytical treatments to find a suitable parametrization of the motion causing nuclear spin relaxation. From the detailed analysis of a 1.5-ns MD trajectory of ubiquitin solvated in a box of water, the basic motional processes affecting backbone spin relaxation were

* To whom correspondence should be addressed. Prof. Rafael Brüschweiler, present address Carlson School of Chemistry, Clark University, Worcester, MA 01610. E-mail: rbruschw@black.clarku.edu. Prof. Richard R. Ernst: phone +41 1 632 43 68, fax +41 1 632 12 57, E-mail ernst@nmr.phys.chem.ethz.ch.

‡ Present address Institut de Biologie Structurale, Laboratoire de RMN, 38027 Grenoble cedex 1, France.

(1) Willis, B. T. M.; Pryor, A. W. *Thermal Vibrations in Crystallography*; Cambridge University Press: London, 1975.

(2) Lipari, G.; Szabo, A. *J. Am. Chem. Soc.* **1982**, *104*, 4546−4559; 4559−4570.

(3) Bremi, T.; Brüschweiler, R. *J. Am. Chem. Soc.* **1997**, *119*, 6672−6673.

(4) Vijay-Kumar, S.; Bugg, C. E.; Cook, W. J. *J. Mol. Biol.* **1987**, *194*, 531−544.

(5) Kraulis, P. J. *J. Appl. Crystallogr.* **1991**, *24*, 946−950.

(6) Di Stefano, D. L.; Wand, A. J. *Biochemistry* **1987**, *26*, 7272−7281. Weber. P. L.; Brown S. C.; Mueller, L. *Biochemistry* **1987**, *26*, 7282−7290.

(7) Schneider, D. M.; Dellwo, M. J.; Wand, A. J. *Biochemistry* **1992**, *31*, 3645−3652. Wand, A. J.; Urbauer, J. L.; McEvoy, R. P.; Bieber, R. J. *Biochemistry* **1996**, *35*, 6116−6125.

(8) (a) Tjandra, N.; Feller, S. E.; Pastor, R. W.; Bax A. *J. Am. Chem. Soc.* **1995**, *117*, 12562-12566. (b) Wang, A. C.; Grzesiek, S.; Tschudin, R.; Lodi, P. J.; Bax, A. *J. Biomol. NMR* **1995**, *5*, 376−382. (c) Tjandra, N.; Szabo, A.; Bax, A. *J. Am. Chem. Soc.* **1996**, *118*, 6986−6991. (d) Ottiger, M.; Tjandra, N.; Bax, A. *J. Am. Chem. Soc.* **1997**, *119*, 9825−9830.

(9) Brutscher, B.; Bremi, T.; Skrynnikov, N. R.; Brüschweiler, R.; Ernst, R. R. *J. Magn. Reson.* **1998**, *130*, 346−351.

(10) Bremi, T.; Brüschweiler, R.; Ernst, R. R. *J. Am. Chem. Soc.* **1997**, *119*, 4272−4284.

S0002-7863(98)01017-8 CCC: $15.00
Published on Web 09/11/1998

Figure 1. Schematic representation of the native state of ubiquitin,[4] drawn by using Molscript.[5]

determined and expressed in terms of an analytical motional model. It is found that 76% of the backbone peptide planes are not involved in conformational exchange processes and show predominantly small-amplitude motion. Their relaxation behavior can be described by the recently proposed 3D Gaussian axial fluctuation (GAF) model.[3] Each peptide plane is treated as a rigid entity exhibiting rapid reorientational motion about three orthogonal principal axes with a Gaussian fluctuation distribution. The axis of maximum angular fluctuation turns out to be nearly parallel to the $C^{\alpha}_{i-1}-C^{\alpha}_{i}$ direction. The model, expressed in analytical terms, is applied to experimental T_1 and T_2 data of the $^{13}C'$ and ^{15}N backbone spins and to $\{^1H\}-^{15}N$ NOE data collected at two magnetic field strengths (400 and 600 MHz proton frequency).

Our approach differs from procedures previously proposed for the dynamical interpretation of $^{13}C'$ carbonyl backbone relaxation in proteins. Engelke and Rüterjans[11] used a model-free description assuming identical order parameters for the three CSA principal axes, which is equivalent to assuming isotropic internal motion at the $^{13}C'$ sites. They found for ribonuclease T1 significant discrepancies between the derived $^{13}C'$ and ^{15}N order parameters belonging to the same peptide bond, but no physical explanation was provided. Allard and Härd[12] recognized the importance of dipolar contributions of the neighboring protons to $^{13}C'$ relaxation and the need for separate order parameters for the different interactions. They modeled the backbone motion of the thermostable Sso7d protein by two order parameters for each $^{13}C'$, one describing motion at the backbone $^{13}C'$ site and one describing the (effective) motion of the internuclear vectors to the neighboring protons. Similar to the treatment by Engelke and Rüterjans, their approach assumes isotropic intramolecular motion at the $^{13}C'$ site. Dayie and Wagner[13,14] derived information on the spectral densities of the carbonyl CSA interaction in villin 14T. No interpretation in terms of anisotropic intramolecular motion was undertaken. Zuiderweg and co-workers[15] measured numerous autocorrelated and cross-correlated relaxation rate constants involving ^{15}N and $^{13}C'$ backbone atoms of flavodoxin and determined the associated motional order parameters. Differences in these order parameters were ascribed to anisotropic peptide plane motion, which was modeled in terms of uniaxial restricted diffusion. No attempt was made to interpret the set of relaxation data by a unified motional model.

The remainder of the paper is organized as follows: In section 2, details of the experiments, the simulation, and an analytical description of the 3D GAF motional model are presented. In section 3, the MD trajectory and the experimental data are analyzed, and peptide planes that display 3D GAF dynamics are selected. Their locally anisotropic fluctuation behavior is discussed and compared to the MD results.

2. Materials and Methods

2.1. Sample Preparation. Fully ^{13}C,^{15}N-labeled ubiquitin was kindly provided by A. J. Wand (Buffalo, NY) and purchased from VLI (Southeastern, PA). For optimal consistency, all $^{13}C'$ and ^{15}N relaxation data used for the analysis were measured on a single ubiquitin sample containing 2 mM ubiquitin in 90% H_2O and 10% D_2O at pH 4.7 with a 45 mM sodium acetate buffer. The sample was deoxygenated and sealed in a standard 5-mm NMR sample tube.

2.2. NMR Experiments. NMR experiments were performed on Bruker AMX-600 and DMX-400 spectrometers equipped with triple-resonance (^1H, ^{15}N, ^{13}C) probes and shielded z gradients. The sample temperature was set to 300 K. The 2D ^{15}N T_1 and T_2 relaxation and $\{^1H\}-^{15}N$ NOE experiments were performed at 400 and 600 MHz in a similar way as previously reported on the A state of ubiquitin.[16] Two sets of T_1 experiments were carried out both at 400 and at 600 MHz to estimate statistical errors. In addition, two sets of T_2 measurements were performed in the rotating frame at 600 MHz with spin-locking fields of $|\gamma_N B_1|/2\pi = 1.9$ and 2.6 kHz, respectively. For the $\{^1H\}-^{15}N$ NOE measurements at both magnetic field strengths, three spectra, two with and one without ^1H saturation, were recorded in an interleaved manner. For ^1H saturation during 5 s of the recycle delay, either a windowless WALTZ-16 sequence or a train of 120° pulses with 10-ms intervals was applied. No systematic deviations of the NOEs were found between the two saturation schemes.

2D $^{13}C'$ T_1 and T_2 relaxation experiments were carried out at 400 and 600 MHz using HNCO-type experiments.[12−14,17] The pulse sequences and the parameter settings are given in the Supporting Information. During the mixing time, ^1H and ^{15}N 180° pulse trains were applied in both T_1 and T_2 experiments, and selective Gaussian $^{13}C^{\alpha}$ 180° pulses were used in the T_1 experiment to suppress both cross-relaxation between $^{13}C'$ and surrounding spins and cross correlation effects between $^{13}C'$ CSA and dipolar interactions ($^{15}N-^{13}C'$, $^1H-^{13}C'$, $^{13}C^{\alpha}-^{13}C'$). Statistical errors were estimated from two sets of T_1 experiments at 400 MHz and three sets of T_1 experiments at 600 MHz. One set of T_2 experiments was performed at 400 MHz using a spin-lock field strength of 1.7 kHz. At 600 MHz, a spin-lock experiment with a rf field strength of 2.7 kHz was compared with a CPMG experiment using a train of selective $^{13}C'$ 180° pulses every 500 μs. No systematic deviation between the two experiments was found.

2.3. Extraction of Relaxation Data. The data were processed with the FELIX program version 95.0 (Biosym

(11) Engelke, J.; Rüterjans, H. *J. Biomol. NMR* **1997**, *9*, 63−78.
(12) Allard, P.; Härd, T. *J. Magn. Reson.* **1997**, *126*, 48−57.
(13) Dayie, K. T.; Wagner, G. *J. Magn. Reson. Ser. B* **1995**, *109*, 105−108.
(14) Dayie, K. T.; Wagner, G. *J. Am. Chem. Soc.* **1997**, *119*, 7797−7806.
(15) Fischer, M. W. F.; Zeng, L.; Pang, Y.; Hu, W.; Majumdar, A.; Zuiderweg, E. R. P. *J. Am. Chem. Soc.* **1997**, *119*, 12629−12642.
(16) Brutscher, B.; Brüschweiler, R.; Ernst, R. R. *Biochemistry* **1997**, *36*, 13043−13053.
(17) Zeng, L.; Fischer, M. W. F.; Zuiderweg, E. R. P. *J. Biomol. NMR* **1996**, *7*, 157−162.

Technologies). Prior to 2D Fourier transformation, the time domain data were zero-filled in the t_2 dimension to 2048 complex points and multiplied with a cosine bell window. For the ^{15}N relaxation experiments, zero-filling was applied in the t_1 dimension to 1024 real points, followed by multiplication with a cosine-bell window. For the ^{13}C′ relaxation experiments, a mirror-image linear prediction procedure[18] was applied along the constant time t_1 dimension, which was followed by zero-filling to 1024 real points and multiplication with a Kaiser window. The resonance assignments were taken from Wang et al.[8b] Peak intensities were extracted from 2D spectra using a local grid search routine for each cross peak. T_1 and T_2 values were determined by fitting the measured peak heights to the monoexponential function $I(T) = I_0 \exp(-T/T_{1,2})$ with two fit parameters, $T_{1,2}$ and the peak intensity I_0 at mixing time $T = 0$. Representative decay curves for ^{13}C′ T_1 and T_2 measurements are shown in the Supporting Information. The $\{^1$H$\}-^{15}$N steady-state NOE values were determined from the ratios of the measured cross-peak intensities in the presence (I_{sat}) and absence (I_{unsat}) of proton saturation: $\mathrm{NOE}^{meas} = I_{sat}/I_{unsat}$.

2.4. Relaxation Theory. Spin relaxation of the ^{15}N and ^{13}C′ nuclei is dominated by dipolar (D) and chemical shift anisotropy (CSA) interactions. Analytical expressions relating dipolar and CSA T_1 contributions and the heteronuclear NOE to power spectral density functions $J(\omega)$ are given in ref 19 and in the Supporting Information. The corresponding expressions for T_2 relaxation are given below. The dipolar contribution of spin j to $T_{2,i}^{-1}$ of spin i is

$$\left(\frac{1}{T_{2,i}}\right)_D = \frac{1}{40}\left(\frac{\mu_0}{4\pi}\right)^2\left(\frac{h}{2\pi}\right)^2\gamma_i^2\gamma_j^2\langle r_{ij}^{-3}\rangle^2\{4J_{\mu\mu}(0) + 3J_{\mu\mu}(\omega_i) + J_{\mu\mu}(\omega_j - \omega_i) + 6J_{\mu\mu}(\omega_j) + 6J_{\mu\mu}(\omega_j + \omega_i)\} \quad (1)$$

where $J_{\mu\mu}(\omega)$ with $\mu = (ij)$ is the autocorrelated spectral density function of the internuclear vector $\boldsymbol{r}_{ij}$.[19] γ_i, γ_j are the gyromagnetic ratios of the spins i and j, and ω_i, ω_j are the corresponding Larmor frequencies. h is Planck's constant, and μ_0 is the magnetic field constant. The CSA contribution to transverse relaxation of spin i is

$$\left(\frac{1}{T_{2,i}}\right)_{CSA} = \frac{1}{90}\omega_i^2\{\delta_x{}^2[4J_{xx}(0) + 3J_{xx}(\omega_i)] + \delta_y{}^2[4J_{yy}(0) + 3J_{yy}(\omega_i)] + 2\delta_x\delta_y[4J_{xy}(0) + 3J_{xy}(\omega_i)]\} \quad (2)$$

The parameters δ_x and δ_y are defined by $\delta_x = \delta_{xx} - \delta_{zz}$ and $\delta_y = \delta_{yy} - \delta_{zz}$, where δ_{xx}, δ_{yy}, δ_{zz} are the principal values of the CSA tensor. $J_{xx}(\omega)$, $J_{yy}(\omega)$ are the autocorrelated spectral densities of the CSA principal axes x and y, and $J_{xy}(\omega)$ is the corresponding cross-correlated spectral density.[19]

It is well-known that conformational exchange processes in the microsecond to millisecond range, that modulate the isotropic chemical shifts, also contribute to $T_{2,i}^{-1}$.[20,21] Since peptide planes exhibiting such chemical exchange processes cannot be characterized by a 3D GAF model alone, they were excluded from further analysis. A straightforward method[16] to identify these peptide planes uses a comparison between the ^{15}N T_2 values and the inverse cross-relaxation rate constant $1/\Gamma_{N,NH}$ induced by cross-correlated relaxation between the ^{15}N$-^1$H dipolar interaction and the ^{15}N chemical shift anisotropy tensor:[9]

$$\Gamma_{N,NH} = \frac{1}{30}\omega_N\left(\frac{\mu_0}{4\pi}\right)\left(\frac{h}{2\pi}\right)\gamma_i\gamma_j\langle r_{ij}^{-3}\rangle\{\delta_x(4J_{NH,x}(0) + 3J_{NH,x}(\omega_N)) + \delta_y(4J_{\mathrm{NH},y}(0) + 3J_{NH,y}(\omega_N))\} \quad (3)$$

$J_{NH,x}$ and $J_{NH,y}$ are the spectral densities related to the cross-correlation functions between the NH vector and the principal axes x and y of the ^{15}N CSA tensor, respectively. $\Gamma_{N,NH}$ leads to differential transverse ^{15}N relaxation of the two multiplet components belonging to the α and β states of the ^1J-coupled H^N spin. Modulations of the ^{15}N chemical shift equally affect both multiplet components and, therefore, do not lead to differential relaxation, provided that the $^1J_{\mathrm{NH}}$ coupling is constant which can be safely assumed.[22]

2.5. 3D Gaussian Axial Fluctuation (GAF) Model. The autocorrelated and cross-correlated spectral density functions can be expressed in terms of the 3D GAF model. From the MD simulation, it follows that 3D GAF internal motion is independent of and much faster than the overall tumbling motion. Furthermore, the ^{15}N relaxation data suggest that the overall tumbling is in good approximation isotropic (vide infra), consistent with ref 8a. Under these conditions, the spectral density functions entering the expressions for the relaxation parameters can be parametrized as[2,9]

$$J_{\mu\nu}(\omega) = S_{\mu\nu}^2\frac{2\tau_c}{1 + (\omega\tau_c)^2} + \{P_2(\cos\theta_{\mu\nu}) - S_{\mu\nu}^2\}\frac{2\tau_{eff,\mu\nu}}{1 + (\omega\tau_{eff,\mu\nu})^2} \quad (4)$$

where μ and ν refer to a dipolar director or a CSA tensor principal axis. The effective correlation time $\tau_{eff,\mu\nu}$ is given by $\tau_{eff,\mu\nu}^{-1} = \tau_c^{-1} + \tau_{int,\mu\nu}^{-1}$, where $\tau_{\mathrm{int},\mu\nu}$ is the correlation time of the internal autocorrelation or cross-correlation function

$$\mathrm{C}_{\mu\nu}^{\mathrm{int}}(t) = \frac{4\pi}{5}\sum_{m=-2}^{2}\langle Y_{2m}(\mathbf{e}_\mu^{mol}(0))Y_{2m}^*(\mathbf{e}_\nu^{mol}(t))\rangle \quad (5)$$

The unit vector $\mathbf{e}_\mu^{mol}(t)$ points along the principal axis μ expressed in a molecular frame which is affected exclusively by the overall rotational diffusion. The Legendre polynomial $P_2(\cos\theta_{\mu\nu})$ of the angle $\theta_{\mu\nu}$ between two principal axes μ and ν enters because of the relation $P_2(\cos\theta_{\mu\nu}) = C_{\mu\nu}^{int}(0) = (4\pi/5)\sum_{m=-2}^{2}\langle Y_{2m}(\mathbf{e}_\mu^{mol})Y_{2m}^*(\mathbf{e}_\nu^{mol})\rangle$, with the normalized second rank spherical harmonics Y_{2m}. For all autocorrelated processes ($\mu = \nu$), one finds $P_2(\cos(0)) = 1$, and for cross-correlation contributions between two principal axes of the same CSA tensor, $P_2(\cos(\pi/2)) = -1/2$. For the 3D GAF motion, the order parameters $S_{\mu\nu}^2$ are given by[3]

$$S_{\mu\nu}^2 = \frac{4\pi}{5}\sum_{l,k,k',m,m'=-2}^{2}(-i)^{k-k'}\exp\left\{-\frac{\sigma_\alpha^2(k^2 + k'^2)}{2} - \sigma_\beta^2 l^2 - \frac{\sigma_\gamma^2(m^2 + m'^2)}{2}\right\} \times d_{kl}^{(2)}\left(\frac{\pi}{2}\right)d_{k'l}^{(2)}\left(\frac{\pi}{2}\right)d_{mk}^{(2)}\left(\frac{\pi}{2}\right)d_{m'k'}^{(2)}\left(\frac{\pi}{2}\right)Y_{2m}(\boldsymbol{e}_\mu^{pp})Y_{2m'}^*(\boldsymbol{e}_\nu^{pp}) \quad (6)$$

where $\boldsymbol{e}_\mu^{pp} = (\theta_\mu, \varphi_\mu)$ defines the direction of the principal axis μ of an interaction tensor in the $\boldsymbol{e}_\alpha$, $\boldsymbol{e}_\beta$, $\boldsymbol{e}_\gamma$ frame rigidly attached

(18) Zhu, G.; Bax, A. *J. Magn. Reson.* **1990**, *90*, 405−410.

(19) Appendix of reference 10. Note that in ref 10, chemical shielding anisotropy principal values σ_{xx}, σ_{yy}, σ_{zz} were used, while in the present work chemical shift anisotropy principal values δ_{xx}, δ_{yy}, δ_{zz} are employed.

(20) McConnell, H. M. *J. Chem. Phys.* **1958**, *28*, *430*.

(21) Deverell, C.; Morgan, R. E.; Strange, J. H. *Mol. Phys.* **1970**, *18*, 553.

(22) Brüschweiler, R.; Ernst, R. R. *J. Chem. Phys.* **1992**, *96*, 1758−1766.

to the peptide plane (pp). $d^{(2)}_{kl}(\pi/2)$ are the reduced Wigner matrix elements evaluated at the angle $\pi/2$.[23] σ_α, σ_β, σ_γ are the standard deviations (expressed in radians) of the fluctuations about the principal axes $\boldsymbol{e}_\alpha$, $\boldsymbol{e}_\beta$, $\boldsymbol{e}_\gamma$. $S^2_{\mu\nu}$ corresponds to the plateau value of the internal correlation function $C^{int}_{\mu\nu}(t)$ of eq 5. Below, it will be shown that, for peptide planes exhibiting 3D GAF motion, the correlation times $\tau_{int,\mu\nu}$ are in the sub-50-ps range, which is consistent with the MD simulation results. This causes the second term of eq 4 to be small, and thus the $\tau_{int,\mu\nu}$ values have only little influence on the relaxation parameters.

Equations 4 and 6 provide a convenient way to determine the influence of 3D GAF motion on autocorrelated and cross-correlated relaxation parameters, or, conversely, they allow the determination of the 3D GAF parameters from experimental data as described in the following. In contrast to the treatment of Fischer et al.,[15] where a variety of peptide plane order parameters is determined before attempting a physical interpretation, our treatment aims at a direct extraction of the 3D GAF parameters from the relaxation data. Equation 6 allows calculation of order parameters from the fitted 3D GAF motional parameters (see section 3.6). The effect of weakly anisotropic overall tumbling is mentioned in section 3.5.

2.6. Generation of Molecular Dynamics Trajectory. The coordinates of the X-ray structure of ubiquitin[4] in the Brookhaven Protein Data Bank (file 1ubq) were used for the starting conformation of the MD simulation. All protons were added in their standard geometric positions using the CHARMM program.[24] The resulting structure was then energy-minimized in vacuo and immersed in a cubic box of a side length of 46.65 Å, containing a total of 2909 explicit water molecules. The simulation was performed with the CHARMM force field version 24b2 under periodic boundary conditions with an integration time step in the Verlet algorithm of 1 fs. The SHAKE algorithm[25] was applied to all bond lengths involving a hydrogen atom. A cutoff of 8 Å was used for nonbonded interactions. Truncation was done with a shifting function for electrostatic interactions with a dielectric constant $\epsilon = 1$ and a switching function for van der Waals interactions. The temperature was set to 300 K, and after an equilibration of 500 ps, snapshots were stored in intervals of 1 ps, leading to a total of 1500 conformations for the 1.5-ns simulation time. The snapshots were then postprocessed by a mass-weighted least-squares difference rotation and translation of the protein backbone atoms with respect to a reference conformation at 750-ps simulation time. In this way, overall rotational and translational diffusion of the molecule that occurs during the simulation is eliminated, yielding atomic coordinates for each snapshot in the same molecular reference frame.

2.7. Processing of Trajectory. The axis directions and fluctuation amplitudes of the 3D GAF model were determined from the trajectory as described in ref 3. Three orthogonal unit vectors, $\boldsymbol{e}_1(t)$, $\boldsymbol{e}_2(t)$, and $\boldsymbol{e}_3(t)$, were rigidly attached to the peptide plane. The orthonormal equilibrium orientations are denoted by $\boldsymbol{e}^0_1$, $\boldsymbol{e}^0_2$, and $\boldsymbol{e}^0_3$. The time-dependent unit vectors were linearly averaged over the whole trajectory. Diagonalization of the product matrix of these averaged vectors $M_{ij} = \langle \boldsymbol{e}_i \rangle^T \langle \boldsymbol{e}_j \rangle$ ($i, j = 1, 2, 3$) by the transformation $\boldsymbol{R}^T\boldsymbol{M}\boldsymbol{R}$ yields the principal axis directions of the fluctuation tensors $\boldsymbol{e}_\alpha$, $\boldsymbol{e}_\beta$, and $\boldsymbol{e}_\gamma$ as $\boldsymbol{R}\boldsymbol{e}^0_1$, $\boldsymbol{R}\boldsymbol{e}^0_2$, and $\boldsymbol{R}\boldsymbol{e}^0_3$. If the angular fluctuation amplitudes about these axes, σ_α σ_β, and σ_γ, are much smaller than π and their distributions are Gaussian, they can be determined by the relationships[3]

$$\sigma^2_\alpha = \frac{1}{2}\left(\log\frac{\lambda_1}{\lambda_2\lambda_3}\right),\ \sigma^2_\beta = \frac{1}{2}\left(\log\frac{\lambda_2}{\lambda_1\lambda_3}\right),\ \sigma^2_\gamma = \frac{1}{2}\left(\log\frac{\lambda_3}{\lambda_1\lambda_2}\right) \quad (7)$$

where λ_1, λ_2, and λ_3 are the eigenvalues of the matrix $\boldsymbol{M}$.

The fluctuation amplitudes were also obtained directly from the trajectory by an alternative method:[26] The fluctuation amplitudes are calculated for each of the 1500 snapshots by aligning the instantaneous peptide plane axes $\boldsymbol{e}_\alpha(t)$, $\boldsymbol{e}_\beta(t)$, and $\boldsymbol{e}_\gamma(t)$ by a transformation with their corresponding equilibrium directions. The transformation is accomplished by three successive rotations of the average peptide-plane frame: (i) rotation by the angle α about the axis $\boldsymbol{e}_\alpha$, (ii) rotation by β about the axis $\boldsymbol{e}_\beta$, and (iii) rotation by γ about the axis $\boldsymbol{e}_\gamma$. Due to the smallness of each of these rotations, the order of their application is not crucial. The resulting distributions of the fluctuations about all three axes with their standard deviations were determined. For all peptide planes with dominant 3D GAF motion, the fluctuation amplitudes obtained by the two methods are in good agreement. Conversely, agreement between the two procedures is a useful indicator for the dominance of the 3D GAF motion of the peptide plane under consideration.

3. Results and Discussion

3.1. Analysis of MD Trajectory. The rapid small-amplitude motion of each peptide plane is described by a reorientational principal axis system, characterizing the motion in terms of distribution functions and time constants with respect to these axes. Such a description is preferred over a characterization in terms of fluctuations in backbone dihedral angle space $\{\varphi_i, \psi_i\}$. As is well-known,[27] the fluctuations of the dihedral angles ψ_{i-1} and φ_i are significantly correlated for rigid peptide planes. However, the large deviations of the correlation coefficients $\rho\psi_{i-1}\varphi_i$ from -1 demonstrate the dependence of the dihedral angular motion also on the motion of adjacent peptide planes.[3]

The peptide planes are labeled and numbered by the amino acid residue that contributes the nitrogen atom. The plane of a (non-proline) peptide bond i contains the atoms $^{15}N_i$, $^1H^N_i$, $^{13}C'_{i-1}$, and O_{i-1}. For each of the 72 non-proline peptide planes in ubiquitin, the reorientational probability distributions obtained from the 1500 snapshots of the trajectory were analyzed. It is found that the motion of 57 non-proline peptide planes involves predominantly 3D Gaussian axial fluctuations. In Figure 2a, results are shown for the representative plane of Ile 30. Nearly all peptide planes located in the α helix or in one of the β strands belong to this group. The effective internal correlation times τ_{int} of the 3D GAF motion is for most of the 57 peptide planes well below 20 ps.

The remaining 15 peptide planes belonging to residues in the loop regions including Thr 7 to Lys 11, Gly 35, Ile 36, Gly 47, Gly 53, Arg 54, and the flexible C-terminus, Arg 72 to Gly 76, show additional jump processes on slower time scales. This leads either to bimodal angular distributions with two dominant conformations (see Figure 2b for peptide plane Leu 8) or to asymmetric distributions due to exchange between a larger number of sites. They were excluded from further analysis (see Table 1).

The interpretation of the motion of a peptide plane by a 3D GAF model *does not* infer that the plane is reorienting in a

(23) Zare, R. *Angular Momentum*; Wiley-Interscience: New York, 1988; Table 3.1, p 89.

(24) Brooks, R. B.; Bruccoleri, R. E.; Olafson, B. D.; States, D. J.; Swaminathan, S.; Karplus, M. *J. Comput. Chem.* **1983**, *4*, 187.

(25) Ryckaert, J. P.; Cicotti, G.; Berendsen, H. J. C. *J. Comput. Phys.* **1977**, *23*, 327−341.

(26) Bremi, T. Ph.D. Thesis No. 12240, ETH Zürich, 1997.

(27) Levy, R. M.; Karplus, M. *Biopolymers* **1979**, *18*, 2465.

Table 1. Exclusion of Peptide Planes Whose Motion Cannot Be Described by a 3D GAF Model Both in Experiment and in Simulation

reason for exclusion	excluded planes	remaining planes
proline residues	Pro 19, Pro 37, Pro 38	72
slow motion apparent in MD trajectory	Thr 7 to Lys 11, Gly 35, Ile 36, Gly 47, Gly 53, Arg 54, Arg 72 to Gly 76	57
NMR relaxation not available[a]	Ile 13, Asp 21, Glu 24, Ala 28, Gln 31, Gly 53, Leu 67, Leu 69, Arg 72, Leu 73	50
slow motion apparent in relaxation data[b]	Leu 8, Thr 9, Gly 10, Lys 11, Asn 25, Asp 52, Gln 62, Arg 74, Gly 75, Gly 76	47
poor fits by 3D GAF model	Gln 2, Ile 23	45

[a] Excluded peptide planes show either spectral overlap or very weak signals (see section 3.2). [b] Excluded peptide planes show either low NOE values or short T_2 relaxation times due to conformational or chemical exchange (see section 3.2).

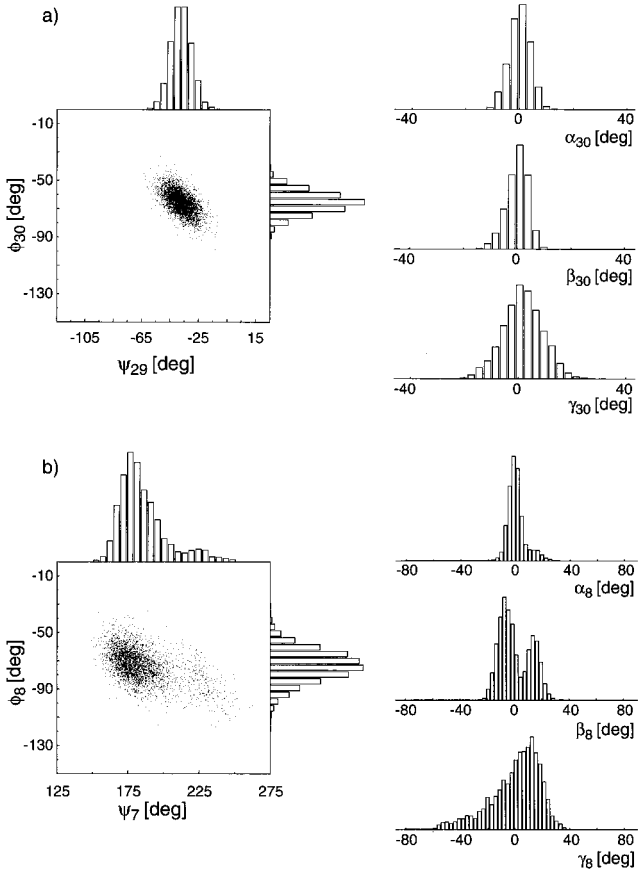

Figure 2. Backbone dihedral angle distributions and peptide plane reorientational probability distributions about the axes $\boldsymbol{e}_\alpha$, $\boldsymbol{e}_\beta$, $\boldsymbol{e}_\gamma$ in ubiquitin derived from the 1.5-ns molecular dynamics simulation in water at 300 K. (a) Probability distributions of Ile 30, exhibiting a unimodal nearly Gaussian behavior. (b) Probability distributions of Leu 8, exhibiting muiltimodal and asymmetric behavior. Peptide plane motion of Leu 8 cannot be described solely by a 3D GAF model.

strictly 3D harmonic potential. 3D GAF motion rather reflects backbone dynamics of the entire protein associated with high-amplitude modes with a collective character.[28] It results from the cumulative effect of projections of a large number of these modes on the individual peptide plane fragments.

The degree of nonplanarity expressed by the dihedral angle ω_i, defined by the atoms $-C^\alpha_{i-1}-C'_{i-1}-N_i-C^\alpha_i-$ of each peptide bond, was determined from the MD trajectory. The average value of ω_i is for all peptide planes near 180° (177°), and the average standard deviation is ±6.8°, which is largely independent of the amino acid type and the secondary structure. The ω_i fluctuations are statistically independent of the superimposed 3D GAF motions and show correlation times that are up to a factor 5 shorter. Thus, an appropriate reference frame

(28) Brüschweiler, R. *J. Chem. Phys.* **1995**, 102, 3396−3403.

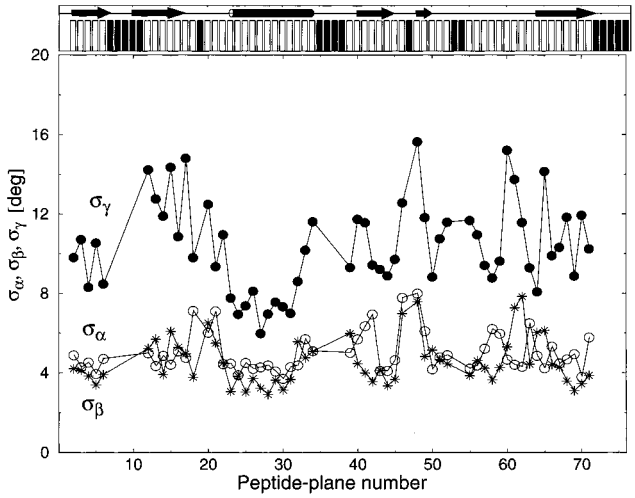

Figure 3. MD reorientational fluctuation amplitudes of the peptide planes of ubiquitin about the principal axes $\boldsymbol{e}_\alpha$, $\boldsymbol{e}_\beta$, $\boldsymbol{e}_\gamma$ as functions of the peptide plane number. The 3D GAF fluctuation amplitudes σ_α (○) σ_β (*), and σ_γ (●) were extracted from the 1.5-ns MD trajectory by using eq 7. The secondary structure is indicated at the top.

for the 3D GAF amplitudes is the effective peptide plane with an averaged ω_i angle.

The directions of the principal axes of the 3D GAF motion and the fluctuation amplitudes were extracted according to eq 7. σ_α, σ_β, and σ_γ are plotted in Figure 3 for the 57 peptide planes. Numerical values are given in the Supporting Information. All 57 peptide planes show a significant degree of intramolecular motional anisotropy, with the largest fluctuation about the axis $\boldsymbol{e}_\gamma$ that is nearly in the peptide plane and parallel to the $C^\alpha_{i-1}-C^\alpha_i$ axis: the average angle to the $C^\alpha_{i-1}-C^\alpha_i$ axis is 7°. Axial symmetry of the fluctuation ellipsoid with equal fluctuation amplitudes about axes $\boldsymbol{e}_\alpha$ and $\boldsymbol{e}_\beta$ ($\sigma_\alpha = \sigma_\beta$) is fulfilled to a good approximation for nearly all peptide planes, as is visible in Figure 3.

3.2 Analysis of Experimental Relaxation Data. The experimental relaxation data of 62 peptide planes were analyzed. No relaxation data were extracted for the remaining 13 peptide bonds belonging (i) to Pro 19, Pro 37, and Pro 38 due to the absence of NH protons, (ii) to Glu 24 and Gly 53 exhibiting peaks with low sensitivity caused by line broadening, and (iii) to Ile 13, Asp 21, Ala 28, Gln 31, Leu 67, Leu 69, Arg 72, and Leu 73 due to cross-peak overlaps in the $^{15}N-^{1}H$ HSQC spectrum (see Table 1). The relaxation data for the two B_0-field strengths are shown in Figure 4 as functions of the peptide plane number. A table with the experimental ^{15}N T_1, T_2, and NOE and $^{13}C'$ T_1 and T_2 values at 400 and 600 MHz is contained in the Supporting Information. Comparison of repeated relaxation measurements yields the following estimates for the statistical uncertainties: 1.5% for ^{15}N T_1's at 400 and 600 MHz, 2% for ^{15}N T_2's at 600 MHz, 4% for ^{15}N NOE's at 400 MHz, 2.5% for ^{15}N NOE's at 600 MHz, 2.5% for $^{13}C'$ T_1's at 400

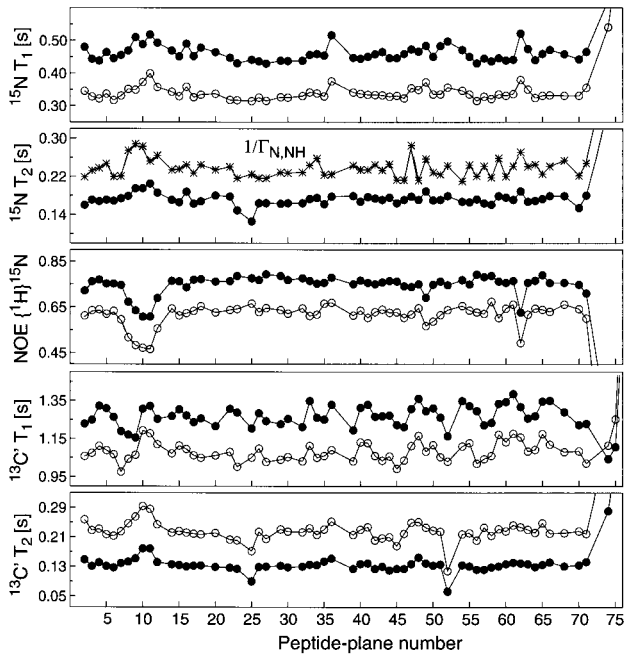

Figure 4. Backbone ^{15}N T_1, T_2, {^{1}H}−^{15}N NOE, and ^{13}C′ T_1, T_2 relaxation data of ubiquitin as functions of the backbone peptide plane number. Relaxation data were measured at two B_0 field strengths, corresponding to the proton resonance frequencies 400 (○) and 600 MHz (●) at 300 K. Significant conformational exchange contributions to ^{15}N T_2 data can be identified by comparison with the inverse ^{15}N−^{1}H dipole−CSA cross-correlation rate constants $1/\Gamma_{N,NH}$ at 600-MHz proton frequency (see text) indicated by ∗ in the second panel.

MHz, 2% for ^{13}C′ T_1's at 600 MHz, 5% for ^{13}C′ T_2's at 400 MHz, and 3% for ^{13}C′ T_2's at 600 MHz.

The peptide planes Leu 8, Thr 9, Gly 10, Lys 11, and Gln 62, which belong to loop regions, and the peptide planes Arg 74, Gly 75, and Gly 76, forming the C-terminus of ubiquitin, show ^{15}N NOE values below 0.52 at 400 MHz and below 0.68 at 600 MHz, which are significantly smaller than those of other peptide planes, which are in the range between 0.52 and 0.67 at 400 MHz and between 0.68 and 0.79 at 600 MHz. This reflects the presence of additional large-amplitude internal motions at slower time scales which cannot be modeled solely by a 3D GAF motion of their peptide planes. These eight peptide planes are excluded from further analysis (see Table 1).

Peptide planes involved in conformational exchange processes were also excluded (Table 1). These comprise peptide planes 25 and 52, which show significantly reduced ^{13}C′ T_2 values (see Figure 4). The same effect is also apparent when comparing the ^{15}N T_2 values at 600 MHz with ^{15}N−^{1}H CSA dipole cross-correlation data obtained from CT-HSQC experiments[8c] (see section 2.4), which are also shown in Figure 4. The absence of a similar anomaly for the peptide plane Asn 25 in $1/\Gamma_{N,NH}$ indicates that the anomaly in ^{15}N T_2 is caused by conformational exchange. This leaves a remainder of 47 peptide planes whose relaxation-active small-amplitude motion can be modeled by a 3D GAF motion.

3.3. Spin Relaxation Mechanisms in the Peptide Plane. The dominant relaxation-active interactions and their principal axis orientations with respect to the peptide plane frame are depicted in Figure 5. Since the interactions probe different directions, their relaxation contributions yield complementary information on the rigid-body motion of the peptide plane. The relative orientations of the interactions relevant for ^{15}N and ^{13}C′

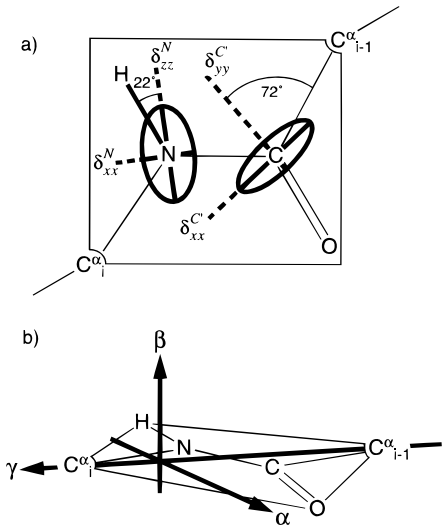

Figure 5. (a) Orientations of the dipolar ^{15}N−^{1}H interaction and chemical shift anisotropy tensors of ^{13}C′ and ^{15}N in the peptide plane. The ^{15}N CSA tensor corresponds to the model compound Boc-Gly-Gly-[^{15}N]Gly-OBz, determined by Hiyama et al.,[30] with the principal values $\delta_{xx}^N = -58.3$ ppm, $\delta_{yy}^N = -51.3$ ppm, $\delta_{zz}^N = 109.6$ ppm. The ^{13}C′ CSA tensor is taken from the model compound [1-^{13}C′]glycyl-Gly-HCl, determined by Stark et al.,[31] with the principal values $\delta_{xx}^{C'} = -74.4$ ppm, $\delta_{yy}^{C'} = -7.4$ ppm, $\delta_{zz}^{C'} = 81.8$ ppm. (b) Definition of the reference coordinate system $\boldsymbol{e}_\alpha$, $\boldsymbol{e}_\beta$, $\boldsymbol{e}_\gamma$ fixed to the peptide plane as used throughout this work. The principal axes directions of the relevant spin interactions, expressed in this frame, are given in Table 2.

relaxation and the relative magnitude of their contributions are given in Table 2.

With regard to ^{15}N relaxation, the standard model-free analysis considers only the dipolar ^{15}N−^{1}H and the ^{15}N CSA relaxation and describes the intramolecular motion by the order parameter S_{NH}^2. One finds, however, that also the ^{15}N−^{13}C′ and ^{15}N−^{13}C$^\alpha$ dipolar relaxations lead to measurable contributions (see upper part of Table 2). They can rigorously be taken into account within the more comprehensive 3D GAF model.

For the backbone ^{13}C′ spins, CSA relaxation is dominant, but dipolar contributions have also to be considered.[12] Even at 600 MHz proton resonance the dipolar contributions are nonnegligible, as is shown in the lower part of Table 2. The largest dipolar contributions to ^{13}C′ relaxation originate from the directly bonded ^{13}C$^\alpha$ and from close protein protons. While the motion of the in-plane dipolar ^{13}C′−^{13}C$^\alpha$ and ^{13}C′−^{1}H^N interactions can be described by the 3D GAF model, the internuclear out-of-plane ^{13}C′−^{1}H$^\alpha$ and ^{13}C′−^{1}H$^\beta$ vectors are influenced also by other types of motion. The influence of all protons, except ^{1}H^N of the same peptide plane, was accounted for by an isotropic dipolar leakage term, which can be expressed[12] as the dipolar relaxation contribution of a virtual proton at an effective distance r_{eff}. This effective distance was calculated for all ^{15}N and ^{13}C′ nuclei in ubiquitin from the energy-minimized X-ray structure. The r_{eff} values for ^{15}N range from 1.72 to 1.87 Å and for ^{13}C′ from 1.69 to 1.90 Å.

3.4. Extraction of 3D GAF Motional Parameters from the Experimental Data. The experimental data of the 47 peptide planes considered were evaluated to determine their 3D GAF fluctuation amplitudes. Based on the MD analysis that showed nearly axially symmetric fluctuation ellipsoids for almost all peptide planes, it was assumed throughout the analysis that $\sigma_\alpha = \sigma_\beta \equiv \sigma_{\alpha\beta}$. The order parameters $S_{\mu\nu}^2$ of eq 6 are then determined for each peptide plane by a pair of $\sigma_{\alpha\beta}$, σ_γ values. Additional parameters entering the spectral densities (eq 4) are

Table 2. Relevant Parameters for Dipolar and CSA Interaction Strengths and Their Contributions to Relaxation of the Backbone ^{15}N and $^{13}C'$ Nuclei, Assuming Isotropic Overall Tumbling with a Correlation Time $\tau_c = 4.03$ ns and Intramolecular 3D GAF Motion of the Peptide Plane

			contributions to $1/T_1$ (%)		
relaxation-active interaction	geometrical and CSA parameters	$(\theta, \varphi)^f$ (deg)	at 400 MHz	at 600 MHz	$S^2_{\mu\mu}{}^i$
$^{15}N-H$	1.02 Å[c]	(101.3, 180)	81.1[g]	70.4[g]	0.81
^{15}N-$^{13}C'$	1.35 Å (0.03)[d]	(138.4, 0)	2.2[g]	1.8[g]	0.86
^{15}N-$^{13}C^\alpha$	1.47 Å (0.03)[d]	(14.4, 0)	1.4[g]	1.1[g]	0.91
$^{15}N-H^{rest}$	1.80 Å (0.03)[e]		3.3[g]	2.9[g]	(1)[j]
^{15}N CSA[a]					
δ_{xx}	−58.3 ppm	(33.3, 180)			0.88
δ_{yy}	−51.3 ppm	(90, 90)	12.0[g]	23.8[g]	0.80[k]
δ_{zz}	109.6 ppm	(123.3, 180)			0.83
$^{13}C'-^{13}C^\alpha_{i-1}$	1.52 Å (0.03)[d]	(159.6, 180)	12.4[h]	11.8[h]	0.90
$^{13}C'-^{13}C^\alpha_i$	2.49 Å[d]	(12.3, 180)	0.6[h]	0.6[h]	0.91
$^{13}C'-^{15}N$	1.35 Å (0.03)[d]	(138.4, 0)	5.5[h]	3.5[h]	0.86
$^{13}C'-H^N$	2.06 Å[d]	(66.9, 180)	8.0[h]	4.6[h]	0.82
$^{13}C'-H^{rest}$	1.82 Å (0.03)[e]		21.3[h]	11.8[h]	(1)[j]
$^{13}C'$ CSA[b]					
δ_{xx}	−74.4 ppm	(2.3, 0)			0.91
δ_{yy}	−7.4 ppm	(92.3, 0)	52.2[h]	67.7[h]	0.80[l]
δ_{zz}	81.8 ppm	(90, 90)			0.80

[a] The principal values and principal axis orientations of the ^{15}N CSA tensor were taken from ref 30. The angle between the CSA *z* axis and the $^{15}N-^1H$ bond vector is 22° (see also Figure 5). [b] The principal values and principal axis orientations of the $^{13}C'$ CSA were taken from ref 31. The angle between the CSA *y* axis and the $^{13}C{=}O$ bond is 13° (see also Figure 5). [c] The $^{15}N-^1H$ bond length was set to the standard value of 1.02 Å. [d] The average bond lengths and their standard deviations given in parentheses were determined from the MD trajectory (see text). [e] A virtual distance between the ^{15}N and $^{13}C'$ nuclei and all protons outside of the peptide plane was calculated for all peptide planes using the energy-minimized X-ray structure.[4] The average value with standard deviation is given. [f] θ, φ are the polar angles of the corresponding spin interaction in the peptide plane frame defined in Figure 5. [g] The contributions are given as percentage of the ^{15}N overall relaxation rate constants $1/T_1 = 3.21$ s^{-1} (400 MHz) and 2.22 s^{-1} (600 MHz), assuming a 3D GAF motion with $\sigma_{\alpha\beta} = 7°$ and $\sigma_\gamma = 14°$, $\tau_c = 4.03$ ns, and $\tau_{int} = 2$ ps. [h] The contributions are given as percentage of the $^{13}C'$ overall relaxation rate constants $1/T_1 = 0.88$ s^{-1} (400 MHz) and 0.73 s^{-1} (600 MHz), assuming a 3D GAF motion with $\sigma_{\alpha\beta} = 7°$ and $\sigma_\gamma = 14°$, $\tau_c = 4.03$ ns, and $\tau_{int} = 2$ ps. [i] The order parameter $S^2_{\mu\mu}$ has been computed for $\sigma_{\alpha\beta} = 7°$ and $\sigma_\gamma = 14°$ according to eq 6. [j] A static approximation ($S^2 = 1$) was assumed to calculate the contribution of the protons outside of the peptide plane since these interactions cannot be modeled by a 3D GAF motion. [k] The order parameter for the cross-correlation function between the *y* and *z* principal axes is $S^2_{yz} = -0.38$. [l] The order parameter for the cross-correlation function between the *y* and *z* principal axes is $S^2_{yz} = -0.35$.

the overall tumbling correlation time τ_c and the correlation times $\tau_{int,\mu\nu}$. For simplicity, we assume that the internal correlation times are isotropic; i.e., in a given peptide plane, $\tau_{int,\mu\nu} = \tau_{int}$ for all pairs $\mu, \nu = \alpha, \beta, \gamma$. This leads to a description of the motion of each peptide plane by the four model parameters $\sigma_{\alpha\beta}$, σ_γ, τ_c, τ_{int}.

The average bond lengths and bond angles were extracted for a number of representative peptide planes from the MD trajectory by averaging over the 1500 snapshots, except for the N−H distance that was set to the standard value of $r^{eff}_{NH} = 1.02$ Å, which has often been used in previous analyses.[7,8a] It is significantly higher than the value obtained from the MD trajectory: $\langle r_{NH} \rangle = 0.997$ Å. Note that r^{eff}_{NH} is an effective distance that reflects averaging by rapid local stretching and bending motion of the N−H bond, $r^{eff}_{NH} = \{S_{bend} \langle r^{-3}_{NH} \rangle_{stretch}\}^{-1/3}$, including also zero-point vibrational effects.[29] The value for r^{eff}_{NH} might need to be modified in the future when more precise information from solid-state NMR and from quantum calculations is available.

It is possible that the CSA tensors vary with the amino acid type, with the presence of hydrogen bonds, and with the local backbone ψ_{i-1} and φ_i dihedral angles. In principle, it is conceivable to extract all CSA parameters by fitting a sufficiently large number of relaxation measurements. The presently available measurements do not permit such a general approach, and the CSA tensors were taken from solid-state NMR studies of small peptide fragments: The ^{15}N CSA tensor of Boc-Gly-Gly-[^{15}N]Gly-OBz was determined by Hiyama et al.[30] and the $^{13}C'$ CSA tensor of [1-^{13}C]glycyl-Gly-HCl by Stark et al.[31] The selected $^{13}C'$ CSA tensor is similar to other experimental tensors,[32a] while for ^{15}N CSA tensors larger variations are observed.[32b] It should be noted that the CSA tensors determined by solid-state NMR correspond to tensors that are partially averaged due to intramolecular motion. Considering this fact, we introduced ^{15}N and $^{13}C'$ CSA scaling factors λ_N and λ_C, which isotropically upscale the experimental CSA tensors. The global scaling factor λ_C was used as a free parameter in the fitting procedure. The exact knowledge of the ^{15}N CSA tensor is less crucial than that of the $^{13}C'$ tensor, since at field strengths corresponding to 400 and 600 MHz proton resonance, ^{15}N relaxation is dominated by dipolar relaxation. The experimental value for the ^{15}N CSA tensor of $\Delta\delta = \delta_{||} - \delta_\perp \cong 164$ ppm[30] (assuming an axially symmetric tensor) was upscaled by a fixed value of $\lambda_N = 1.07$ to compensate for the motional averaging in the solid-state NMR study. This corresponds to a rigid molecule value of $\Delta\delta \cong 176$ ppm, which is used in the following for all peptide planes. Similar values have been applied in other NMR studies.[8d,33]

Instead of using a uniform scaling factor, λ_C, in the fitting procedure, one might consider individually scaling the different $^{13}C'$ CSA tensors by scaling factors $\lambda_{C,i}$ for each peptide plane. This would allow one to partially account for the structural

(29) Brüschweiler, R. *J. Am. Chem. Soc.* **1992**, *114*, 5341−5344.
(30) Hiyama, Y.; Niu, C.; Silverton, J. V.; Bavoso, A.; Torchia, D. A. *J. Am. Chem. Soc.* **1988**, *110*, 2378−2383.
(31) Stark, R. E.; Jelinski, L. W.; Ruben, D. J.; Torchia, D. A.; Griffin, R. G. *J. Magn. Reson.* **1983**, *55*, 266−273.
(32) (a) Oas, T. G.; Hartzell, C. J.; McMahon, T. J.; Drobny, G. P.; Dahlquist, F. W. *J. Am. Chem. Soc.* **1987**, *109*, 5956−5962. Separovic, F.; Smith, R.; Yannoni; C. S.; Cornell, B. A. *J. Am. Chem. Soc.* **1990**, *112*, 8324−8328. Teng, Q.; Iqbal, M.; Cross, T. A. *J. Am. Chem. Soc.* **1992**, *114*, 5312−5321. (b) Hartzell, C. J.; Whitfield, M.; Oas, T. G.; Drobny, G. P. *J. Am. Chem. Soc.* **1987**, *109*, 5966−5969. Oas, T. G.; Hartzell, C. J.; Dahlquist, F. W.; Drobny, G. P. *J. Am. Chem. Soc.* **1987**, *109*, 5962−5966.
(33) Tjandra, N.; Wingfield, P.; Stahl, S.; Bax, A. *J. Biomol. NMR* **1996**, *8*, 273−284.

dependence of the CSA tensors. Although a sufficient number of relaxation measurements was available, the fitting procedure turned out to be unstable due to a strong correlation of $\lambda_{C,i}$ with the motional parameters $\sigma_{\alpha\beta}$, σ_γ.

For each peptide plane i, an overall tumbling correlation time $\lambda_{C,i}$ was extracted from the ^{15}N data alone by a standard model-free analysis, fitting the parameters $\tau_{c,i}$, $\tau_{int,i}$, and S_i^2 to the experimental ^{15}N T_1, NOE (400 and 600 MHz), and T_2 (600 MHz) data. Averaging over all 47 residues (see above) yields $\tau_c = 4.03$ ns, which is well comparable with a previously determined value of 4.09 ns obtained under similar experimental conditions.[8a]

The fluctuation amplitudes $\sigma_{\alpha\beta}$, σ_γ and the internal correlation time τ_{int} were fitted to the nine experimental parameters ^{15}N T_1, T_2, and NOE and ^{13}C′ T_1 and T_2 at 400 and 600 MHz for each of the 47 peptide planes. The peptide planes of Gln 2 at the N-terminus of ubiquitin and Ile 23 were excluded (see Table 1) due to a large least-square fit error (four times larger than the average one). The relaxation data of Gln 2 reflect increased flexibility of the N-terminus which cannot be described by 3D GAF motion. The scaling factor λ_C for the ^{13}C′ CSA tensor was determined as a global fit parameter for the remaining 45 peptide planes. A value $\lambda_C = 1.083 \pm 0.004$ was obtained that reflects the motional averaging of the CSA tensor in the solid-state measurement,[31] since $\lambda_C > 1.0$. The overall tumbling correlation time τ_c was kept fixed at 4.03 ns. The fit results for the fluctuation amplitudes are shown in Figure 6 as functions of the peptide plane number. A table with the numerical values for all fit parameters and a figure with the internal correlation times are given in the Supporting Information. For all peptide planes, the internal correlation time τ_{int} converges in the fitting procedure to small values $\tau_{int} \leq 30$ ps, consistent with the MD results, rendering the relaxation data largely insensitive to τ_{int}. Nearly all of the 45 peptide planes exhibit 3D GAF motion with a substantial degree of anisotropy, with $\sigma_\gamma > \sigma_{\alpha\beta}$. Thus, the dominant axial fluctuations of the peptide planes take place about the $\boldsymbol{e}_\gamma$ axis connecting C^α_{i-1} and C^α_i. On average, the experimentally determined fluctuation amplitudes, given in Figure 6, are about a factor 1.4 ($\sigma_{\alpha\beta}$) and a factor 1.6 (σ_γ) larger than the ones observed in the MD trajectory (see Figure 3).

3.5. Uncertainty Estimates of Fit Parameters. Experimental Random Errors. To estimate the influence of experimental random errors on the fitted fluctuation amplitudes $\sigma_{\alpha\beta}$ and σ_γ, a Monte Carlo error analysis was performed. In a series of 60 runs, random Gaussian errors with the experimentally determined standard deviations (see section 3.2) were added to the experimental relaxation data. For each of the 60 data sets, a simultaneous fit of the individual fluctuation amplitudes of the 45 peptide planes and of a global scaling factor λ_C for the ^{13}C′ CSA tensors was performed. The resulting errors of the fluctuation amplitudes are indicated as error bars in Figure 6; the numerical values are given in the Supporting Information.

Dependence of ^{13}C′ CSA Tensors on Secondary Structure. To further investigate the structural dependence of the ^{13}C′ CSA tensor, we divided the 45 peptide planes into the three categories "α helix", "β sheet", and "other". We then fitted individual scaling factors for each category and obtained $\lambda_C^{helix} = 1.076 \pm 0.008$, $\lambda_C^{sheet} = 1.070 \pm 0.010$, and $\lambda_C^{other} = 1.096 \pm 0.010$. The resulting fluctuation amplitudes of the 45 peptide planes are given as a separate figure in the Supporting Information. The similarity of the three scaling factors seems to confirm that the ^{13}C′ CSA tensors of ubiquitin vary only slightly. An investigation is currently in progress that evaluates the possibility of using density functional theory (DFT) for obtaining a reliable estimate

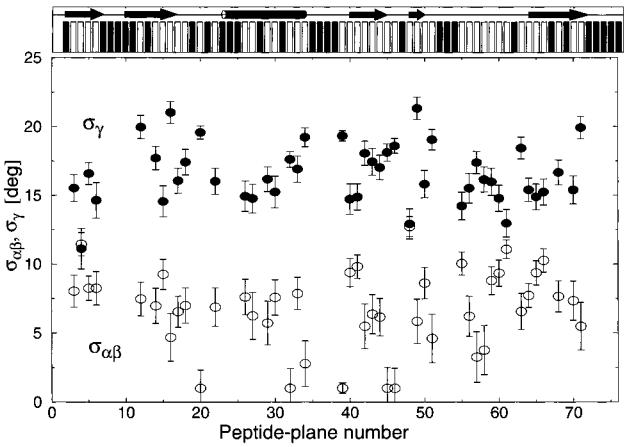

Figure 6. Fit of the 3D GAF model (eqs 4 and 6) to the experimental data consisting of nine autorelaxation parameters for each peptide plane represented in Figure 4. The optimized parameter set consists of a global scaling factor, λ_C, for the principal values of the ^{13}C′ CSA tensor and three parameters, $\sigma_{\alpha\beta}$, σ_γ, and τ_{int}, for each peptide plane. The overall correlation time τ_c was set to 4.03 ns, and the principal values of the ^{15}N CSA tensor, given in Table 2, were upscaled with $\lambda_N = 1.07$ (see text). The optimum scaling factor is $\lambda_C = 1.083$. The optimum values $\sigma_{\alpha\beta}$ (○) and σ_γ (●) are given in the figure for each peptide plane. The error limits of the fitted parameters were determined by a Monte Carlo procedure consisting of 60 fits with random Gaussian errors added to the relaxation parameters according to the experimental standard deviations. The secondary structure is indicated at the top.

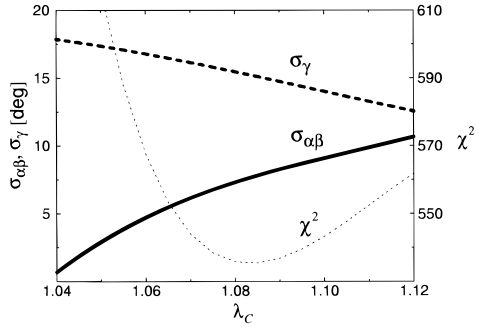

Figure 7. Dependence of the fit parameters $\sigma_{\alpha\beta}$ (solid line) and σ_γ (dashed line) on the global scaling factor λ_C for the ^{13}C′ CSA tensor illustrated for peptide plane Ile 30. The corresponding overall fitting error function χ^2 (sum of the error contributions of all 45 peptide planes) for the global fit of λ_C is given as a dotted line.

of the CSA tensors for different environments of the peptide planes. Preliminary results confirm the limited variation of the anisotropy. The computed anisotropy of the ^{13}C′ CSA tensors of residues located in the α helix and in β strands differs by less than 3%.

Effect of Interaction Strength on Fit Results. In Figure 7, the dependence of the fitted fluctuation amplitudes $\sigma_{\alpha\beta}$ and σ_γ on the global scaling factor λ_C is illustrated for the peptide plane Ile 30. The figure shows that λ_C has a strong influence on the motional anisotropy of the peptide plane defined in section 3.7. λ_C is uniquely defined, as can be seen from the error function of the fit.

Anisotropic Overall Tumbling. In the present analysis, it was assumed that ubiquitin undergoes isotropic overall tumbling (see section 2.5). The tumbling anisotropy of ubiquitin has been determined by Tjandra et al.[8a] to be ≈18 %. An analysis of the influence of an 18% anisotropy of tumbling on the fitted 3D GAF fluctuation amplitudes shows an effect of less than 1° on the fitted fluctuation amplitudes $\sigma_{\alpha\beta}$ and σ_γ, depending on the average peptide plane orientation with respect to the overall

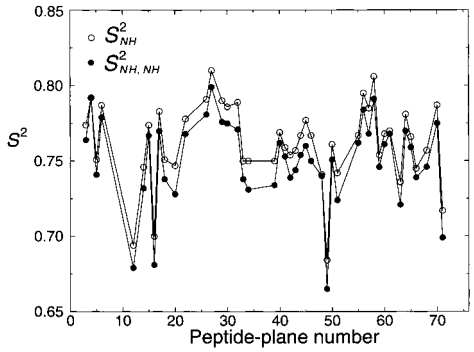

Figure 8. Compatibility of 3D GAF model with a standard ^{15}N model-free analysis. The $S^2_{NH,NH}$ order parameters for the dipolar ^{15}N−^{1}H interaction derived from the 3D GAF model data of Figure 6 and eq 6 (●) are compared with the ^{15}N S^2_{NH} order parameters determined by a model-free analysis from ^{15}N relaxation data at 400 and 600 MHz (○). τ_c was set to 4.03 ns, and an axially symmetric ^{15}N CSA tensor with $\Delta\delta = 176$ ppm was assumed. Additional relaxation contributions from other protons (assuming a rigid molecular frame), from the ^{15}N−^{13}C′ dipolar interaction (assuming an averaged order parameter $S^2_{NC'}$, = 0.83), and from the ^{15}N−^{13}C$^{\alpha}$ dipolar interaction (assuming an averaged order parameter $S^2_{NC\alpha} = 0.89$) were also included in the model-free analysis.

tumbling diffusion tensor. A maximal effect occurs for a symmetry axis of the rotational diffusion tensor that is perpendicular to the average peptide plane.

3.6. Comparison between the 3D GAF Analysis and a ^{15}N Model-Free Analysis. Based on the results of the 3D GAF analysis and by using eq 6, it is possible to calculate order parameters $S^2_{\mu\nu}$ for arbitrary pairs of spin interactions within the peptide plane. In Table 2, the order parameters for different interactions are given for the following values of the fluctuation amplitudes: $\sigma_{\alpha\beta} = 7°$, $\sigma_\gamma = 14°$. The calculated order parameters are largest for the dipolar ^{15}N−^{13}C$^{\alpha}$ and ^{13}C′−^{13}C$^{\alpha}$ interactions, which are less modulated by the dominant fluctuation about the C^{α}_{i-1}−C^{α}_{i} axis than, for example, the ^{15}N−^{1}H interaction.

The order parameters $S^2_{NH,NH}$ of the dipolar ^{15}N−^{1}H interaction were calculated for all 45 evaluated peptide planes using eq 6, together with the fitted 3D GAF fluctuation amplitudes from Figure 6. In Figure 8, these values are compared with order parameters obtained directly from a standard model-free analysis of the ^{15}N T_1, T_2, and NOE data at both field strengths. These order parameters are termed here S^2_{NH}. Figure 8 shows a good overall agreement between the order parameters $S^2_{NH,NH}$ and S^2_{NH} calculated by the two approaches. It illustrates the compatibility of the 3D GAF analysis with the model-free description. The systematic offset between the two sets is due to the assumption in the model-free analysis of an equal order parameter S^2_{NH} for the dipolar NH and for the ^{15}N CSA interactions. This is, however, only justified for isotropic internal motion or for an axially symmetric CSA tensor with the unique axis collinear to the NH vector. These assumptions are not realistic (see Table 2) and are not required for the 3D GAF analysis.

A model-free analysis based exclusively on ^{15}N relaxation data yields neither axial fluctuation amplitudes nor information on the anisotropy of intramolecular peptide plane motion. Such additional information is provided by the complementary ^{13}C′ relaxation data that form an integral part of the 3D GAF analysis.

3.7. Anisotropy of Peptide Plane Dynamics. The 3D GAF fluctuation amplitudes extracted from the MD analysis and from the relaxation data yield insight into the degree of anisotropy of the peptide plane motions. A convenient measure for the degree of anisotropy is the "anisotropy factor",

$$\frac{\Delta\sigma}{\bar{\sigma}} = \frac{\sigma_\gamma - \sigma_{\alpha\beta}}{(\sigma_\gamma + 2\sigma_{\alpha\beta})/3} \tag{8}$$

reflecting the difference between reorientational motion about the C^{α}_{i-1}−C^{α}_{i} axis and motion about the orthogonal axes, weighted by the average fluctuation amplitude. The anisotropy factors for all peptide planes obtained from the MD trajectory and from the experimental results are given in the Supporting Information.

We note here that there are qualitative and quantitative differences between the results of the experimental NMR relaxation study and the MD simulation. The quantitative differences in the fluctuation amplitudes become apparent by comparing Figures 3 and 6. The experimental fluctuation amplitudes are, on average, larger than those in the MD simulation. Reasons for these discrepancies may be suspected in the choice of not accurately known geometric parameters in the data evaluation. On the other hand, it is also conceivable that the CHARMM force field used is slightly too stiff, leading to low fluctuation amplitudes.

The sets of peptide planes showing large-amplitude, non-3D GAF motion apparent in the experimental data and the MD simulation are not identical. This particularly concerns the peptide planes of Asn 25 and Glu 62, showing non-3D GAF motion in the experimental data but 3D GAF motion in the simulation. The peptide planes of Thr 7, Gly 35, Ile 36, Gly 47, and Arg 54 exhibit non-3D GAF motion only in the simulation. Due to the restricted length of the trajectory, there is some uncertainty concerning the statistical significance of jump processes that led in section 3.1 to the exclusion of peptide planes from the 3D GAF analysis. There is also little correlation between the residue-specific 3D GAF fluctuation amplitudes in the experimental and the MD data. In this context, one should remember that even a rather long MD trajectory, covering more than 1 ns, represents in essence an "extended snapshot" of the long-term motion of the protein and does not comprehensively cover the ensemble conformations relevant for the experimental results. For this reason, no agreement in all details can be expected, even for a "perfect" force field.

3.8. Correlation with Secondary structure. An attempt was made to correlate the fluctuation amplitudes with the secondary structure elements of native ubiquitin in Figure 1, which are indicated also at the top of Figures 3 and 6. Average fluctuation amplitudes were calculated separately for α helical, β sheet, and other regions from the MD trajectory: $\langle\sigma_{\alpha\beta}\rangle_{helix} = 4.1°$, $\langle\sigma_\gamma\rangle_{helix} = 8.0°$, $\langle\sigma_{\alpha\beta}\rangle_{sheet} = 4.7°$, $\langle\sigma_\gamma\rangle_{sheet} = 11.0°$, $\langle\sigma_{\alpha\beta}\rangle_{other} = 5.3°$, and $\langle\sigma_\gamma\rangle_{other} = 11.0°$ (see also Figure 4 of the Supporting Information). The central α helix shows a rather homogeneous behavior, with fluctuation amplitudes that are somewhat lower than for the rest of the protein. The loop regions and the β sheet regions are more flexible but do not show significant differences when compared to each other. As described in section 3.1 and Table 1, only peptide planes are taken into account that exhibit an exclusive 3D GAF behavior.

The differences of the experimentally determined fluctuation amplitudes between the three categories are even smaller. The average fluctuation amplitudes are $\langle\sigma_{\alpha\beta}\rangle_{helix} = 5.5°$, $\langle\sigma_\gamma\rangle_{helix} = 16.4°$, $\langle\sigma_{\alpha\beta}\rangle_{sheet} = 7.7°$ and $\langle\sigma_\gamma\rangle_{sheet} = 16.5°$, and $\langle\sigma_{\alpha\beta}\rangle_{other} = 5.8°$, and $\langle\sigma_\gamma\rangle_{other} = 16.8°$. Figure 9 shows the (almost) absent correlation of the experimental parameters $\sigma_{\alpha\beta}$ and σ_γ with the secondary structure elements. Ellipses are shown in the $\sigma_{\alpha\beta}$, σ_γ plane that contain the pairs of values of the planes located

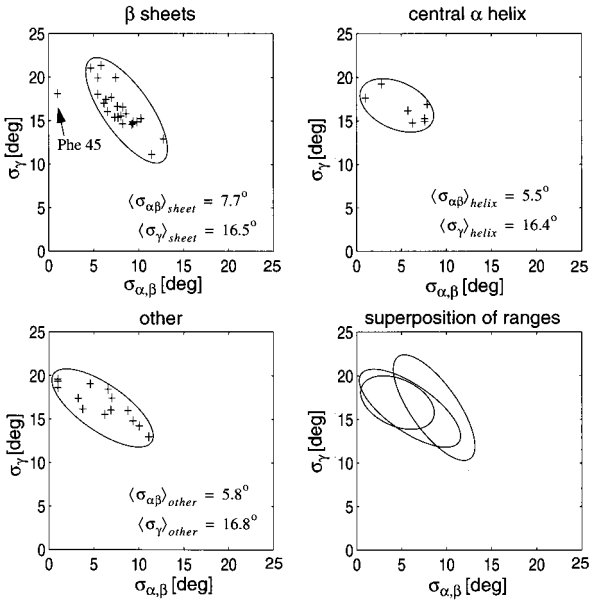

Figure 9. Loci of the pairs of experimental fluctuation amplitudes $\sigma_{\alpha\beta}$, σ_γ for the different peptide planes and their assignment to the three categories "α helix", "β sheet", and "others", indicated by ellipses.

in one of the three categories. It is apparent that the ellipses strongly overlap and miss a characteristic structure-related behavior. On the other hand, there is a significant anticorrelation between $\sigma_{\alpha\beta}$ and σ_γ, leading to similarly inclined ellipses for all three structural elements.

As mentioned above, the absence of a significant correlation of the fluctuation amplitudes with the secondary structure reflects to some extent the fact that the peptide planes with large-amplitude motion have been excluded from the analysis. On the other hand, it demonstrates that the most rigid parts of a globular protein, like ubiquitin, show similar fluctuation amplitudes irrespective of the secondary structure.

4. Conclusion

So far, mostly local order parameters have been used to characterize intramolecular mobility in biopolymers. The authors are convinced that future investigations will concentrate increasingly on the description of the anisotropic motion of entire molecular subunits, such as secondary structural elements, aromatic rings, purine or pyrimidine bases, peptide planes, or methylene groups. Considering these subunits as rigid objects, it is possible to deduce the motional anisotropy of their motion from the autorelaxation and cross-relaxation properties of several observer nuclei rigidly attached to the same fragment.

In this paper, we concentrated on fast-time-scale motional processes exhibited by the rigid backbone peptide planes, which are reflected in $^{13}C'$ and ^{15}N relaxation data. By comparison with an extended MD simulation, those peptide planes were identified and characterized which are dominated by anisotropic 3D Gaussian axial fluctuations. A significantly anisotropic motional behavior was found that depends little on the secondary structure elements. The extracted motional parameters, however, depend critically on the magnitude and orientation of the dipolar and CSA interaction tensors, responsible for relaxation. It is hoped that, in the future, solid-state NMR studies of labeled proteins and refined quantum chemical calculations[34] will provide more accurate information on these tensors and will lead to a better understanding of their dependence on the local environment. This will lead to more accurate and more realistic descriptions of the dynamics of peptide planes and other molecular subunits. Supported by the further developments of NMR and MD methodologies, studies of this type will provide information for a better understanding of the relationship between dynamics and biomolecular function.

Acknowledgment. The authors thank Prof. A. J. Wand for providing ^{13}C,^{15}N-labeled ubiquitin. This work was supported by the Swiss National Science Foundation.

Supporting Information Available: Experimental details, summary of relevant relaxation equations, analysis of molecular dynamics trajectory, and analysis of experimental data (20 pages, print/PDF). See any current masthead page for ordering information and Web access instructions.

JA9810179

(34) Le, H.; Pearson, J. G.; de Dios, A. C.; Oldfield, E. *J. Am. Chem. Soc.* **1995**, *117*, 3800−3807. Sitkoff, D.; Case, D. A. *J. Am. Chem. Soc.* **1997**, *119*, 12262−12273. Woolf, T. B.; Malkin, V. G.; Malkina, O. L.; Salahub, D. R.; Roux, B. *Chem. Phys. Lett.* **1995**, *239*, 186.